HASIL CEK3_60181174

by 60181174 Teknik Kimia

Submission date: 09-Feb-2022 11:26AM (UTC+0700)
Submission ID: 1758258316
File name: Teknik Kimia_60181174_Shinta_Paper 3 - Shinta Amelia.pdf (1.64M)
Word count: 4956
Character count: 25336

ARTICLE IN PRESS

Journal of Environmental Chemical Engineering xxx (xxxx) xxxx

Contents lists available at ScienceDirect

Journal of Environmental Chemical Engineering

journal homepage: www.elsevier.com/locate/jece

Role of the pore structure of Fe/C catalysts on heterogeneous Fenton oxidation

Shinta Amelia[a,b], Wahyudi Budi Sediawan[a], Imam Prasetyo[a,c], Macarena Munoz[d], Teguh Ariyanto[a,c,*]

[a] Department of Chemical Engineering, Faculty of Engineering, Universitas Gadjah Mada, 55281 Yogyakarta, Indonesia
[b] Program of Chemical Engineering, Universitas Ahmad Dahlan, Jl. Prof. Dr. Soepomo, S.H, Umbulharjo, 55164, Yogyakarta, Indonesia
[c] Advanced Material and Sustainable Mineral Processing Research Group, Universitas Gadjah Mada, 55281 Yogyakarta, Indonesia
[d] Seccion Departamental Ingenieria Quimica, Universidad Autonoma de Madrid, Ctra. Colmenar km 15, 28049 Madrid, Spain

ARTICLE INFO

Keywords:
Catalytic oxidation
Dye removal
Iron oxide
Porous carbon

ABSTRACT

The aim of this work is to evaluate the influence of the pore structure of Fe-supported carbon catalysts in heterogeneous Fenton oxidation. For such goal, two types of porous carbons i.e. biomass-derived carbon (BDC) and polymer-derived carbon (PDC) were employed as catalytic supports. Both solids present the same specific surface area (ca. 1300 m^2/g) but a different character of porosity. The former showed a remarkable pore fraction in the range of micropores (< 2 nm) whereas the latter displayed substantial pores in the range of micro- and mesopores (2–5 nm). The Fe_2O_3/carbon catalysts were produced by wet impregnation of iron oxide precursor followed by calcination at 300 °C. Elemental mapping of EDX analysis confirmed the evenly distribution of metal on carbon, which Fe loading was set to 0.5, 1 and 2 wt.%. Remarkably, the specific surface area of the supports remained almost unchanged after the immobilization of iron oxide (below 5% drop). The performance of the catalysts was investigated in the oxidation of methylene blue (MB) under ambient conditions ($[MB]_0 = 20\ mg\ L^{-1}$; $[H_2O_2]_0 = 12.5\ mL\ L^{-1}$; [catalyst] = 125 mg L^{-1}; 30 °C). The experimental data were successfully described by an intraparticle gradient model with first order of reaction of methylene blue and accounting adsorption equilibrium. The mass transfer and reaction parameters showed that the porous structure of the support plays a key role on the oxidation process. Iron oxide dispersed on mesoporous support was more advantageous i.e. featuring a higher reaction rate constant (40% increase in removal capability). Regarding the stability, the mesoporous catalyst maintained its high activity upon four consecutive runs.

1. Introduction

Methylene blue (MB) is a thiazine dye widely used in textile industries. This compound is difficult to degrade naturally due to its low biodegradability, hence it can harm the balance of environment ecosystem. Adsorption method e.g. using porous carbon as the adsorbent is one popular technique in dye removal [1–5]. However, this adsorptive removal only transfers the pollutant compounds to other media or phases. Thus, additional process to treat dye loaded in the porous material might apply which is not desirable from economic and environmental issues. In this context, the application of heterogeneous Fenton oxidation appears as a promising alternative as it allows to degrade completely the organic pollutants [6,7]. This process is based on the decomposition of H_2O_2 by a solid catalyst leading to the formation of hydroxyl radicals, highly reactive species which attack non-selectively most of the organic pollutants. Iron represents the main active phase for this system [8] although other transition metals such as cobalt [9], cerium [10] and niobia [11] have been also investigated. Regarding the catalytic supports, alumina [12], pillared clays [13] or silica [14] have been evaluated but carbon materials are usually regarded as the most promising solids due to their outstanding properties such as good physical and chemical stability, high specific surface areas (500-2000 m^2/g), well developed and different porous structures and variable surface composition [15–17]. The scheme of removal of MB using a heterogenous Fenton reaction is shown in Fig. 1 when using a standard catalyst for Fenton reaction i.e. iron oxide.

Many works in the literature have been devoted to the application of different carbon materials as catalyst supports for heterogeneous Fenton oxidation [7,8,18]. Nevertheless, the influence of the pore structure of these materials on the catalytic performance has not been

* Corresponding author at: Department of Chemical Engineering, Faculty of Engineering, Universitas Gadjah Mada, 55281 Yogyakarta, Indonesia.
E-mail address: teguh.ariyanto@ugm.ac.id (T. Ariyanto).

https://doi.org/10.1016/j.jece.2019.102921
Received 5 October 2018; Received in revised form 8 January 2019; Accepted 23 January 2019

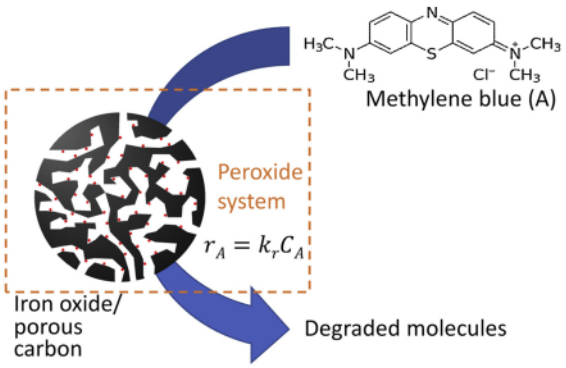

Fig. 1. Schematic of degradation of methylene blue with a help of iron oxide/carbon catalyst and peroxide (For interpretation of the references to colour in this figure legend, the reader is referred to the web version of this article).

investigated in depth so far. The pore structure of carbon plays important roles e.g. for transporting metal precursor and providing area for dispersing active metal. Furthermore, the pore sizes could influence reaction environment inside pores, when a combination of strong adsorption of compound and Fenton reaction happens simultaneously. Therefore, in the end the performance of synthesized catalyst is indirectly influenced by the support. This work is focused on evaluating the effect of pore character of carbon support on the resulting Fenton catalyst and its performance in the degradation of MB. Two different carbon supports have been used for such goal: biomass-derived carbon (BDC, dominant microporous structures) and polymer-derived carbon (PDC, dominant mesoporous structures). PDC is porous carbon prepared by carbonization of synthetic polymer and its pore size can be easily tuned by altering polymeric precursors [16,17,19]. Accordingly, although PDC exhibits a mesoporous structure, it also shows a specific surface area similar to the microporous carbon of BDC (ca. 1300 m^2g^{-1}). Both carbons were employed as catalyst support of iron oxide and the properties of the synthesized catalysts were characterized in detail. To qualitatively describe the performance of the catalytic systems, data of dye removal were evaluated using an intraparticle gradient model accounting methylene blue reaction and adsorption equilibrium. Finally, the stability of the optimum catalyst was studied upon its sequential use in four consecutive runs.

2. Experimental section

2.1. Materials

The carbon supports used in this study were biomass-derived carbon (BDC), available from PT. HOME System Indonesia, and polymer-derived carbon (PDC) synthesized by pyrolysis of phenolic resin. Fe $(NO_3)_3.9H_2O$ (99% purity Merck, Germany) was employed as iron oxide precursor. In the Fenton reaction, methylene blue (95%, Sigma Aldrich, Singapore) was used as target pollutant and H_2O_2 (50% purity) available from Merck, Germany, was used as a hydroxyl radical producer.

2.2. PDC preparation

PDC material was prepared by two steps *i.e.* preparation of phenolic polymer and its subsequent conversion to carbon. The polymeric precursor was composed by resorcinol (R), formaldehyde (F) and cetyltrimethylammonium bromide (CTAB). Methods of polymer preparation and carbonization process are provided elsewhere [16]. In short, solution was prepared by mixing formaldehyde (37%), CTAB (98%), Na_2CO_3 as catalyst (99.9%) and resorcinol (99% purity). All reagents for preparation of polymer were purchased from Merck, Germany. The molar ratio of formaldehyde to resorcinol was fixed to 2.8 (1 mol resorcinol in 0.28 L of formaldehyde solution). Concentration of CTAB and catalyst used were 0.01 M and 6×10^{-5} M, respectively. The mixture was gently stirred till resorcinol formaldehyde polymer was formed. The dried polymer was then carbonized at 850 °C in furnace, with heating rate of 5 °C/minute and under nitrogen atmosphere.

2.3. Catalyst preparation

Iron oxide was loaded onto the porous carbons by a wet impregnation method followed by calcination process. About 2 g of porous carbon was degassed at 150 °C for 2 h. Subsequently, a proper amount of $Fe(NO_3)_3.9H_2O$ dissolved in isopropanol was then added. After evaporation of the solvent, the solid was dried at 60 °C overnight. The calcination process was then carried out at 300 °C in a quartz tubular reactor (ramp rate of 2 °C/min) for 3 h in nitrogen flow. According to the literature, the iron oxide phase produced under these conditions is hematite (α-Fe_2O_3) [20]. The loading of Fe_2O_3 was established at 0.5, 1, and 2 wt.%. The resulting iron oxide-loaded porous carbons were denoted as *X* wt.% Fe_2O_3/type of carbon. For instance, 2% Fe_2O_3/PDC refers to a 2% loading of iron on the polymer-derived carbon.

2.4. Fenton reaction test

A 200 ml of methylene blue solution (20 mg L^{-1}) was placed in a three-neck flask. The solution was stirred at a constant speed of 450 rpm (at a room temperature of 30 °C). Then, a 5 mL H_2O_2 aqueous solution (50%) and 25 mg of Fe_2O_3/C were simultaneously added into the reactor while stirring. Prior the analysis of the reaction sample, the catalyst was separated using a 0.45 µm syringe filter. The concentration of methylene blue was determined by ultraviolet–visible (UV/VIS) spectrophotometer (Shimadzu UV Mini 1240, Japan) at a wavelength of 663 nm.

2.5. Reaction modeling

An intraparticle reaction model was employed to describe the experimental data by generating mass balance in the volume element of a sphere particle. In this model, the MB concentration gradient and reaction within the solid phase are considered. The diffusion of the dye follows the Fick equation of mass transfer and the degradation of this substance within the catalyst is assumed to attend a first reaction order ($r_A = k_r C_A$). The formula of the model is given in the Eq. (1).

$$\frac{\partial^2 C_A}{\partial r^2} + \frac{2}{r}\frac{\partial C_A}{\partial r} - \frac{k_r C_A}{D_e} = \frac{\varepsilon}{D_e}\cdot\frac{\partial C_A}{\partial t} \quad (1)$$

where C_A is the concentration of MB, k_r is the first-order reaction constant, D_e is the effective diffusivity, and ε is the material porosity. Since it is first order in the time (t) and two orders in the radius (r), to solve the equation there are one initial condition and two boundary conditions as shown in Eqs. (2), (3) and (4). Eq. (3) means that at the solid surface and at any time, the diffusion flux has the same amount with the mass transfer flux in the bulk phase. Whereas, Eq. (4) means that the concentration of methylene blue in the center of solid is in a minimum value.

$$C_A(r, 0) = 0 \quad (2)$$

$$-D_e\frac{\partial C_A}{\partial r}(R, t) = k_c\left(C_{AL} - \frac{1}{H}C_A(R, t)\right) \quad (3)$$

$$\frac{\partial C_A}{\partial r}(0, t) = 0 \quad (4)$$

where k_c is the mass transfer coefficient and H is the Henry constant. The parameters i.e. k_r, k_c, D_e and H were obtained by fitting the experimental data with least square regression rate approaches.

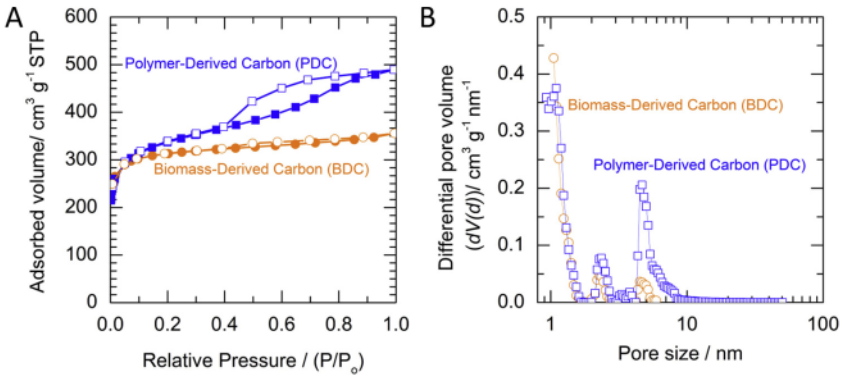

Fig. 2. A) N_2-sorption isotherm (closed symbol: adsorption, open symbol: desorption). (B) pore size distribution of carbon employed as support material.

2.6. Characterization methods

Pore structure of carbon support and iron oxide-loaded carbon (Fe_2O_3/C) was characterized by N_2-sorption analysis (Nova 2000, Quantachrome, USA). Multipoint Brunauer–Emmett–Teller (BET) with a positive value of constant physical parameters was employed to determine the specific surface area [21]. The pore size distributions (PSDs) were evaluated using Quenched Solid Density Functional Theory (QSDFT) model from equilibrium adsorption-desorption isotherm for slit/cylindrical pores [22]. The morphology of material was observed by scanning electron microscope (SEM) of JSM-6510 LA (JEOL, Japan). The elemental mapping of iron oxide in carbon was investigated using SEM-energy dispersive X-ray spectroscopy (SEM-EDX).

3. Results and discussion

3.1. Pore structure of the carbon supports

The textural properties of the carbon supports were characterized using low-temperature nitrogen physisorption analysis. Fig. 2A displays the sorption isotherms. BDC exhibits a characteristic isotherm for microporous material (Type I) while PDC displays a typical adsorption for micro- and mesoporous material (a combination of Type I and IV) according to the International Union of Pure and Applied Chemistry (IUPAC) classification [21]. A substantial N_2-uptake capacity of both carbons indicate that highly porous material is present. The pore size distributions (PSDs) calculated with the QSDFT model (Fig. 2B) showed that BDC and PDC display different pore characteristics. BDC showed a remarkable pore fraction in the range micropores (< 2 nm). On other hand, PDC displays substantial pores in range of micro- and mesopores (2–5 nm).

Textural properties (specific surface area (SSA), pore volume, microporosity and average pore size) of BDC and PDC are summarized in Table 1. The pristine material (before immobilization of iron oxide) is named as 0 wt.% Fe_2O_3. The SSA of both BDC and PDC is nearly the same (ca. 1300 m^2/g). It is important to highlight that these solids could compete with porous carbons synthesized from other polymeric materials which are typically in the range of 1000-2000 $m^2 g^{-1}$ [19]. The pore volume of PDC (0.8 $cm^3 g^{-1}$) is larger than BDC (0.6 $cm^3 g^{-1}$) due to a portion of mesopore volume. Mean pore diameter of carbon was evaluated and is given in Table 1. PDC and BDC exhibit ca. 2.5 and 1.8 nm average pore size, respectively. Overall from the porosity analysis, it can be concluded that BDC and PDC feature a similar surface area, but different pore sizes, thus they are suitable for the study of effect of porosity on dye removal.

3.2. Characterization of Fe_2O_3/BDC and Fe_2O_3/PDC catalysts

Fe_2O_3/C catalysts was prepared by impregnation of the iron oxide precursor followed by calcination. To investigate the distribution of the active material on the carbon surface, SEM-EDX was carried out. Fig. 3 displays SEM image of Fe_2O_3/carbon and its Fe elemental mapping by EDX (BDC, see Fig. 3A and B; PDC, see Fig. 3C and D). Based on SEM images, the surface of BDC is rougher than that of PDC. This likely relates to elemental composition and polymeric network of the carbon precursor [16,23]. The yellow/green color of the elemental mapping indicates the presence of Fe on the carbon surface. In both solids, iron was homogeneously distributed, which is in good agreement with the low content of active metal immobilized on the supports [24].

The pore structure of iron oxide-loaded porous carbon was characterized using N_2-sorption to investigate influences of iron oxide loading on the carbon structural properties. The characterization results

Table 1
Pore structural properties of iron oxide/C.

Catalyst	Specific surface area (SSA[a]) [m^2/gram]	Micropore surface portion (% S_{mic}[b]) [%]	Total pore volume (V_T[c]) [cm^3/gram]	Micropore volume portion (% V_{mic}[b]) [%]	Mean pore diameter (d_v[d]) [nm]
BDC support					
0 wt.% Fe_2O_3	1320	92.12	0.60	75.50	1.82
0.5 wt.% Fe_2O_3	1236	92.55	0.56	77.30	1.81
2 wt.% Fe_2O_3	1165	92.36	0.55	76.90	1.89
PDC support					
0 wt.% Fe_2O_3	1285	79.14	0.80	50.75	2.48
0.5 wt.% Fe_2O_3	1093	76.85	0.72	48.61	2.62
2 wt.% Fe_2O_3	1195	78.74	0.76	51.71	2.53

[a] Multipoint BET with a positive value of constant physical parameters.
[b] Determined by *t-plot* method.
[c] Pore volume at 0.995 P/P_o.
[d] Calculated with $d_v = \frac{4V_T}{SSA}$.

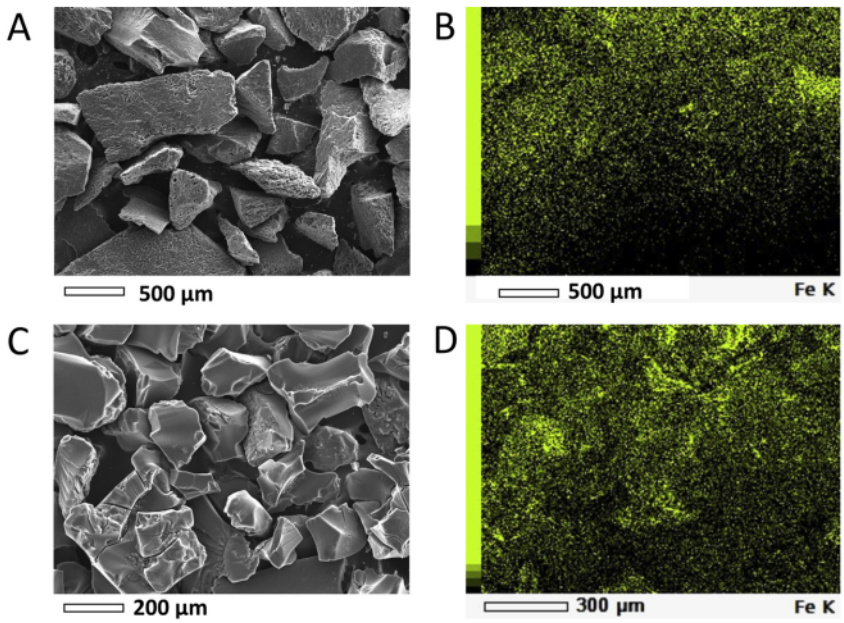

Fig. 3. The SEM image and elemental mapping of Fe on 2 wt. % of Fe_2O_3 on carbon: BDC (A, B) and PDC (C, D).

are shown in Table 1. It can be seen that for both carbon supports, the specific surface area and pore volume were slightly decreased (5–12%) when introducing Fe_2O_3 at different loadings. On the other hand, there was no significant difference on the mean pore size between pristine and loaded carbon. This implies that Fe loading does not change the pore sizes, and thus, the minor decrease of SSA is likely induced by mass addition from non-porous Fe_2O_3 material.

3.3. Catalytic performance

Prior catalytic test, a blank experiment with MB and H_2O_2 in the absence of catalyst was performed to evaluate the possible role of H_2O_2 as direct oxidation agent (see Fig. 4A). As observed, no significant decrease of MB was observed after 24 h reaction time. It can be then concluded that H_2O_2 cannot oxidize the dye in the absence of catalyst under the operating conditions tested in this work. A negligible degradation of dye with only using hydrogen peroxide is likely correlated to its low oxidation potential, when hydroxyl radicals are not present [25].

The results obtained in the heterogeneous Fenton oxidation of MB using the own-prepared catalysts (1 wt.% Fe_2O_3) are summarized in Fig. 4B. The experimental data were fitted using the intraparticle gradient model considering first order of reaction for MB degradation and accounting adsorption equilibrium. There is a 70% reduction of dye from polluted water (red color, with catalyst but absence of H_2O_2) when using only adsorptive method of BDC. With addition of peroxide in 1 wt.%/BDC, the Fenton reaction was occurred, and it led to remarkable drop of methylene blue up to 85% at 3 h reaction. This was due to the very strong oxidative properties of the hydroxyl radicals (HO·) produced from hydrogen peroxide and Fe catalyst [26]. The reduction of MB is even better when using 1 wt.%/PDC with almost full degradation of methylene blue at 3 h. This result indicates that porous structure of carbon influences the removal performance and likely mesoporous support give more advantageous.

Fig. 5A displays the degradation of MB using catalysts with different contents of iron oxide in PDC support (0.5, 1, and 2 wt.%). The kinetic rate of methylene **blue** decolorization increases when using a higher oxide loading. To quantitively discuss the performance, the data were fitted using Eq. (1) and the parameters are summarized in Table 2, together with data on BDC support. The kinetic rate of decoloration is

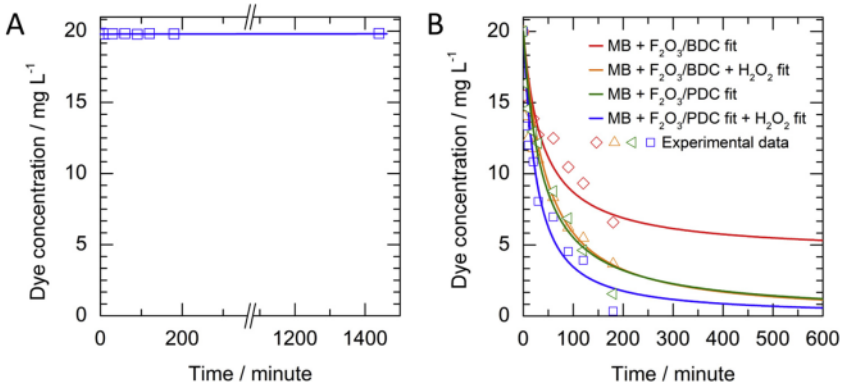

Fig. 4. (A) Concentration profile of methylene blue (MB) in blank Fenton reaction. (B) Concentration profile of methylene blue (MB) in different system during Fenton catalytic testing. Reaction conditions: 25 mg of catalyst (1 wt.% iron on carbon), 200 mL volume, 20 mg L^{-1} dye, 12.5 mL L^{-1} H_2O_2, 450 rpm stir and 30 °C temperature (For interpretation of the references to colour in this figure legend, the reader is referred to the web version of this article).

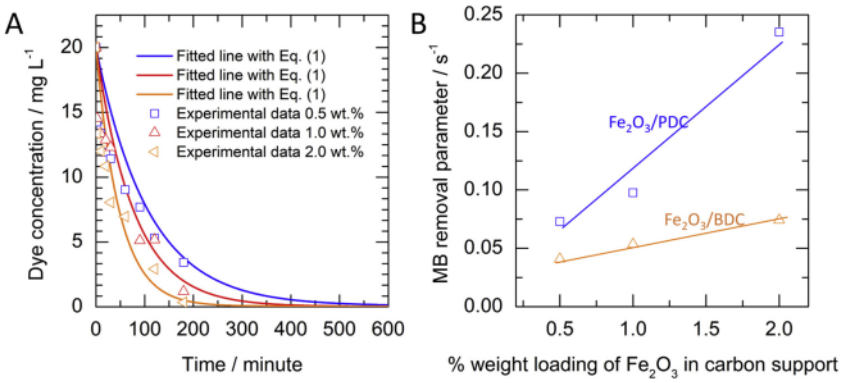

Fig. 5. (A) Concentration profile of methylene blue (MB) at different contents of iron oxide on PDC support. (B) Parameter of kinetic removal of MB using iron oxide dispersed on BDC and PDC. Reaction conditions: 25 mg of catalyst, 200 mL volume, 20 mg L^{-1} dye, 12.5 mL L^{-1} H_2O_2, 450 rpm stir and 30 °C temperature (For interpretation of the references to colour in this figure legend, the reader is referred to the web version of this article).

Table 2
Value of parameters of methylene blue decolorization at various Fe loading. The data fitted using Eq. (1).

Parameter		k_c [m/s]	H	D_e [m^2/s]	$k_r = k_c a_s$ [1/s]
BDC	0.5%	3.2×10^{-3}	14.06	4.2×10^{-10}	0.041
	1%	3.8×10^{-3}	14.73	4.3×10^{-10}	0.054
	2%	3.6×10^{-3}	14.81	4.1×10^{-10}	0.074
PDC	0.5%	8.9×10^{-3}	14.16	6.1×10^{-10}	0.073
	1%	8.3×10^{-3}	14.33	5.9×10^{-10}	0.098
	2%	8.1×10^{-3}	14.79	6.0×10^{-10}	0.235

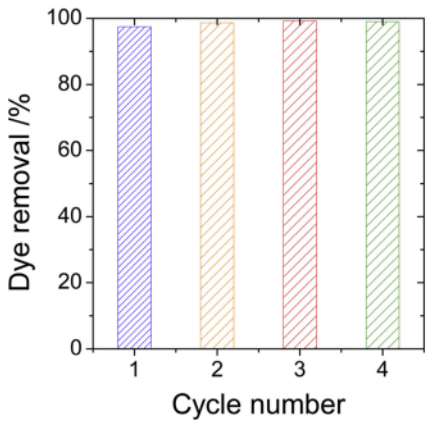

Fig. 6. Durability test showing high reusability of Fe_2O_3/C for dye removal. Reaction conditions: 25 mg of catalyst (1 wt.% iron on carbon), 200 mL volume, 20 mg L^{-1} dye, 15 g L^{-1} H_2O_2, 450 rpm stir, 30 °C temperature and 3 h reaction time.

represented by k_r value. For both carbon supports, the higher Fe loading leads to increase the rate constant. This is likely induced by higher active sites of iron oxide, hence accelerating the degradation of MB. The kinetic rate parameters for iron oxide in BDC and PDC are in the range of 0.04-0.075 s^{-1} and 0.07-0.23 s^{-1}, respectively, hence indicating excellent performances of iron oxide/PDC for MB removal (see Fig. 5B for in graphics). The high performance of iron oxide/PDC is likely supported by larger porosity of the support. The mesoporous structures could give a good system for adsorption of dye on pore surface and reaction of substance with hydroxyl radical which occurred simultaneously [27]. This is further proofed by higher values of mass transfer (k_c) and diffusion coefficient in case of PDC support compared to BDC (see Table 2).

3.4. Recyclability tests of Fe_2O_3/PDC catalyst

To evaluate the reusability of the optimum catalyst (Fe_2O_3/PDC), it was submitted to consecutive oxidation runs. The results obtained are shown in Fig. 6. As can be seen, almost complete removal of the dye (99%) was achieved after 3 h reaction time along the four runs. The good reusability of the catalyst can be favorably compared with previous iron catalysts supported on commercial active carbon materials [8]. The outstanding stability of the mesoporous carbon-based catalyst can be related to the higher efficiency on the removal of the dye adsorbed in the mesopores. In microporous supports, the organic pollutant tends to be strongly adsorbed in the micropores, which can ultimately be blocked and not further available in further uses [28].

4. Conclusion

The influence of the pore structure of the carbon catalytic support in heterogeneous Fenton oxidation of methylene blue has been evaluated. It has been demonstrated that the mesoporous solid is significantly more efficient than the microporous one, obtaining up to 3-fold higher oxidation rates. This outstanding performance was explained by the faster diffusion of H_2O_2 within the mesopores of the carbon material. Remarkably, the mesoporous catalyst Fe_2O_3/PDC showed a high stability, maintaining its activity almost unchanged upon four sequential oxidation runs.

Acknowledgment

The authors would like to thank PT. HOME System Indonesia for a gift of commercial activated carbon.

References

[1] T. Ariyanto, M. Kurniasari, W.T. Laksmana, I. Prasetyo, Pore size control of polymer-derived carbon adsorbent and its application for dye removal, Int. J. Environ. Sci. Technol. (2018) 1–6, https://doi.org/10.1007/s13762-018-2166-0.
[2] M. Aban Tanyildizi, Modeling of adsorption isotherms and kinetics of reactive dye from aqueous solution by peanut hull, Chem. Eng. J. 168 (2011) 1234–1240, https://doi.org/10.1016/j.cej.2011.02.021.
[3] B.H. Hameed, A.T.M. Din, A.L. Ahmad, Adsorption of methylene blue onto bamboo-based activated carbon: kinetics and equilibrium studies, J. Hazard. Mater. 141 (2007) 819–825, https://doi.org/10.1016/j.jhazmat.2006.07.049.
[4] M.F.R. Pereira, S.F. Soares, J.J.M. Olfao, J.L. Figueiredo, Adsorption of dyes on activated carbons: influence of surface chemical groups, Carbon 41 (2003) 811–821, https://doi.org/10.1016/S0008-6223(02)00406-2.
[5] Y.C. Wong, Y.S. Szeto, W.H. Cheung, G. McKay, Adsorption of acid dyes on chitosan - Equilibrium isotherm analyses, Process Biochem. 39 (2004) 693–702, https://doi.org/10.1016/S0032-9592(03)00152-3.
[6] M. Munoz, F.J. Mora, Z.M. de Pedro, S. Alvarez-Torrellas, J.A. Casas, J.J. Rodriguez, Application of CWPO to the treatment of pharmaceutical emerging pollutants in different water matrices with a ferromagnetic catalyst, J. Hazard. Mater. 331 (2017) 45–54, https://doi.org/10.1016/j.jhazmat.2017.02.017.
[7] L. Wang, Y. Yao, Z. Zhang, L. Sun, W. Lu, W. Chen, H. Chen, Activated carbon fibers

as an excellent partner of Fenton catalyst for dyes decolorization by combination of adsorption and oxidation, Chem. Eng. J. 251 (2014) 348–354, https://doi.org/10.1016/j.cej.2014.04.088.

[8] C.S. Castro, M.C. Guerreiro, L.C.A. Oliveira, M. Gonçalves, A.S. Anastácio, M. Nazzarro, Iron oxide dispersed over activated carbon: support influence on the oxidation of the model molecule methylene blue, Appl. Catal. A Gen. 367 (2009) 53–58, https://doi.org/10.1016/j.apcata.2009.07.032.

[9] P.C.C. Faria, D.C.M. Monteiro, J.J.M. Órfão, M.F.R. Pereira, Cerium, manganese and cobalt oxides as catalysts for the ozonation of selected organic compounds, Chemosphere (2008), https://doi.org/10.1016/j.chemosphere.2008.10.016.

[10] M.H.M.T. Assumpção, A. Moraes, R.F.B. De Souza, I. Gaubeur, R.T.S. Oliveira, V.S. Antonin, G.R.P. Malpass, R.S. Rocha, M.L. Calegaro, M.R.V. Lanza, M.C. Santos, Low content cerium oxide nanoparticles on carbon for hydrogen peroxide electrosynthesis, Appl. Catal. A Gen. 411 (2012) 1–6, https://doi.org/10.1016/j.apcata.2011.09.030.

[11] L.C. Oliveira, M. Goncalves, M.C. Guerreiro, T.C. Ramalho, J.D. Fabris, M.C. Pereira, K. Sapag, A new catalyst material based on niobia/iron oxide composite on the oxidation of organic contaminants in water via heterogeneous Fenton mechanisms, Appl. Catal. A (2007) 117–124, https://doi.org/10.1016/j.apcata.2006.09.027.

[12] M. Munoz, Z.M. de Pedro, N. Menendez, J.A. Casas, J.J. Rodriguez, A ferromagnetic γ-alumina-supported iron catalyst for CWPO. Application to chlorophenols, Appl. Catal. B Environ. 136–137 (2013) 0218–0224, https://doi.org/10.1016/j.apcatb.2013.02.002.

[13] S. Navalon, M. Alvaro, H. Garcia, Heterogeneous Fenton catalysts based on clays, silicas and zeolites, Appl. Catal. B Environ. 99 (2010) 1–26, https://doi.org/10.1016/j.apcatb.2010.07.006.

[14] L. Xiang, S. Royer, H. Zhang, J.M. Tatibouët, J. Barrault, S. Valange, Properties of iron-based mesoporous silica for the CWPO of phenol: a comparison between impregnation and co-condensation routes, J. Hazard. Mater. 172 (2009) 1175–1184, https://doi.org/10.1016/j.jhazmat.2009.07.121.

[15] T. Ariyanto, A. Kern, B.J.M. Etzold, G.-R. Zhang, Carbide-derived carbon with hollow core structure and its performance as catalyst support for methanol electrooxidation, Electrochem. Commun. 82 (2017) 12–15, https://doi.org/10.1016/j.elecom.2017.07.010.

[16] I. Prasetyo, T. Rochmadi, Ariyanto, R. Yunanto, Simple method to produce nanoporous carbon for various applications by pyrolysis of specially synthesized phenolic resin, Indones. J. Chem. 13 (2013) 95–100, https://doi.org/10.22146/ijc.21290.

[17] I. Prasetyo, Rochmadi, E. Wahyono, T. Ariyanto, Controlling synthesis of polymer-derived carbon molecular sieve and its performance for CO2/CH4 separation, Eng. J. 21 (2017), https://doi.org/10.4186/ej.2017.21.4.83.

[18] M. Arshadi, M.K. Abdolmaleki, F. Mousavinia, A. Khalafi-Nezhad, H. Firouzabadi, A. Gil, Degradation of methyl orange by heterogeneous Fenton-like oxidation on a nano-organometallic compound in the presence of multi-walled carbon nanotubes, Chem. Eng. Res. Des. 112 (2016) 113–121, https://doi.org/10.1016/j.cherd.2016.05.028.

[19] K. Lenghaus, G. GuangHua Qiao, D.H. Solomon, C. Gomez, F. Rodriguez-Reinoso, A. Sepulveda-Escribano, Controlling carbon microporosity: the structure of carbons obtained from different phenolic resin precursors, Carbon 40 (2002) 743–749, https://doi.org/10.1016/S0008-6223(01)00194-4.

[20] M. Munoz, Z.M. de Pedro, N. Menendez, J.A. Casas, J.J. Rodriguez, A ferromagnetic γ-alumina-supported iron catalyst for CWPO. Application to chlorophenols, Appl. Catal. B Environ. 136–137 (2013) 218–224, https://doi.org/10.1016/j.apcatb.2013.02.002.

[21] M. Thommes, K. Kaneko, A.V. Neimark, J.P. Olivier, F. Rodriguez-Reinoso, J. Rouquerol, K.S.W. Sing, Physisorption of gases, with special reference to the evaluation of surface area and pore size distribution (IUPAC Technical Report), Pure Appl. Chem. 87 (2015), https://doi.org/10.1515/pac-2014-1117.

[22] G.Y. Gor, M. Thommes, K.A. Cychosz, A.V. Neimark, Quenched solid density functional theory method for characterization of mesoporous carbons by nitrogen adsorption, Carbon 50 (2012) 1583–1590, https://doi.org/10.1016/j.carbon.2011.11.037.

[23] H. Sun Choo, L. Chung Lau, A. Rahman Mohamed, K. Teong Lee, Hydrogen sulfide adsorption by alkaline impregnated coconut shell activated carbon, J. Eng. Sci. Technol. 8 (2013) 741–753.

[24] S.H. Joo, S.J. Choi, I. Oh, J. Kwak, Z. Liu, O. Terasaki, R. Ryoo, Ordered nanoporous arrays of carbon supporting high dispersions of platinum nanoparticles, Nature 412 (2001) 169–172, https://doi.org/10.1038/35106621.

[25] J.H. Ramirez, F.J. Maldonado-Hódar, A.F. Pérez-Cadenas, C. Moreno-Castilla, C.A. Costa, L.M. Madeira, Azo-dye Orange II degradation by heterogeneous Fenton-like reaction using carbon-Fe catalysts, Appl. Catal. B Environ. 75 (2007) 312–323, https://doi.org/10.1016/j.apcatb.2007.05.003.

[26] M. Fayazi, M.A. Taher, D. Afzali, A. Mostafavi, Enhanced Fenton-like degradation of methylene blue by magnetically activated carbon/hydrogen peroxide with hydroxylamine as Fenton enhancer, J. Mol. Liq. 216 (2016) 781–787, https://doi.org/10.1016/j.molliq.2016.01.093.

[27] Y. Xiao, J.M. Hill, Impact of pore size on Fenton oxidation of methyl orange adsorbed on magnetic carbon materials: trade-off between capacity and regenerability, Environ. Sci. Technol. 51 (2017) 4567–4575, https://doi.org/10.1021/acs.est.7b00089.

[28] F. Duarte, F.J. Maldonado-Hódar, A.F. Pérez-Cadenas, L.M. Madeira, Fenton-like degradation of azo-dye Orange II catalyzed by transition metals on carbon aerogels, Appl. Catal. B Environ. 85 (2009) 139–147, https://doi.org/10.1016/j.apcatb.2008.07.006.

HASIL CEK3_60181174

ORIGINALITY REPORT

13%	13%	16%	0%
SIMILARITY INDEX	INTERNET SOURCES	PUBLICATIONS	STUDENT PAPERS

PRIMARY SOURCES

1	Shinta Amelia, R. Septiani Muflikhah, Ustinah. "Role of The Concentration of Fe/C Catalysts on Heterogeneous Fenton Degradation Remazol Yellow FG", IOP Conference Series: Materials Science and Engineering, 2021 Publication	4%
2	www.mdpi.com Internet Source	3%
3	link.springer.com Internet Source	3%
4	www.researchgate.net Internet Source	3%

Exclude quotes	On	Exclude matches	< 2%
Exclude bibliography	On		